Chinese Chemical Letters 34 (2023) 107575

Contents lists available at ScienceDirect

Chinese Chemical Letters

journal homepage: www.elsevier.com/locate/cclet

# Erythrocyte membrane encapsulated gambogic acid nanoparticles as a therapeutic for hepatocellular carcinoma

Ruijie Liu[a,1], Li He[b,1], Maoyu Liu[c], Lu Chen[c], Jun Hou[a,*], Jianyou Shi[c,*], Lan Bai[c,*]

[a] Affiliated Hospital of Southwest Jiaotong University/Department of Cardiology, Chengdu Third People's Hospital, Chengdu 610031, China
[b] Department of Pharmacy, Jianyang Chinese Medicine Hospital, Chengdu 641499, China
[c] Personalized Drug Therapy Key Laboratory of Sichuan Province, Department of Pharmacy, Sichuan Academy of Medical Sciences & Sichuan Provincial People's Hospital , School of Medicine, University of Electronic Science and Technology of China, Chengdu 610072, China

ARTICLE INFO

*Article history:*
Received 29 December 2021
Revised 24 May 2022
Accepted 31 May 2022
Available online 3 June 2022

*Keywords:*
Gambogic acid
Erythrocyte membrane
Drug delivery systems
Biomimetic nanoparticles
Hepatocellular carcinoma

ABSTRACT

Gambogic acid (GA) is a potential clinical anticancer drug that can exert antitumor effects *via* various molecular mechanisms. Notwithstanding, GA's low water solubility, poor stability, short half-life, and unavoidable toxic side effects have significantly hampered its clinical application. Erythrocyte membrane-coated nanoparticles (RBCM-NPs) improve drug's physicochemical properties, biocompatibility, and pharmacokinetic behaviors, allowing for long-term drug circulation and passive targeting. In this study, a novel biomimetic drug delivery system (DDS) against hepatocellular carcinoma was prepared by covering RBCM on GPP-NPs (GA-loaded mPEG-PLA NPs) to develop the RBC@GPP-NPs. In comparison to RBCM-free nanoparticles and free GA, RBC@GPP-NPs improved the drug's water solubility, stability, safety, and antitumor activity *in vivo*. We expect that this bionic nanoparticle composite can expand the clinical applicability of GA and provide a feasible solution for the research and development of GA's nano-formulation.



Hepatocellular carcinoma (HCC) is the third leading cause of cancer death worldwide, the fifth most common cancer worldwide, and the most common and fatal primary liver cancer (75%–85%) [1,2]. Pharmacological treatments are irreplaceable in the fight against cancer, where natural compounds play an increasingly important role [3,4]. Gambogic acid (GA), a natural compound with a polyprenylated xanthone structure, is the main active component of gamboge, a widely used Chinese herbal medicine, and is derived from the resin of the *Garcinia Hanburryi* tree in Southeast Asia [5]. GA has significant antitumor activity against multiple cancers, including liver cancer [6,7], lung cancer [8], breast cancer [9], and pancreatic cancer [10]. Especially, GA has better suppression on HCC cells with high expression of UNC119 (uncoordinated 119 or retinal protein 4) [11]. Additionally, our team has also demonstrated that GA can have effective inhibition of proliferation against some liver cancer cells, which stimulated our interest in its further study. Unfortunately, the poor water solubility (less than 0.5 μg/mL) and short half-life of GA (less than 20 min in rats) limit its clinical applications [12,13]. A variety of drug delivery systems (DDS), including the current rapidly evolving bionanosystems, have been designed to overcome these barriers. Cell membrane-coated nano-delivery platforms are simple and adaptable technologies that provide nanoparticles with increased safety and biocompatibility, longer *in vivo* retention time, and enhanced antitumor activity [14–18].

Recently, numerous cell membranes, including platelet membrane [19], macrophage membrane [20], and tumor cell membranes [21], have been employed to improve the biological connectivity and targeting of DDS to cancer cells. The various protein compositions of these membranes endow the nanoparticles with diverse biological functions such as immune escape, prolonged drug circulation time, and enhanced targeting, and help to streamline the tedious bottom-up preparation process [22]. These fruits are inspired by the application of erythrocyte membrane (RBCM).

On one hand, as the first natural membrane donor to receive attention, erythrocytes have the richest cellular source, an exceptionally long *in vivo* circulation time (4 months), and autoimmune regulatory proteins (CD47) located on the cell membrane surface, which allow for a longer retention time of nanoparticles encapsulated in the erythrocyte membrane, effective avoidance of non-self recognition and uptake by macrophages, and long-term drug circulation [23–25]. On the other hand, the preparation process for RBCM-coated NPs (RBCM-NPs) dates back to 2011 and has been very mature so far, during which the RBCM-NPs are widely used to optimize the application of many natural products (curcumin and

* Corresponding authors.
*E-mail addresses:* jun_hou@yeah.net (J. Hou), shijianyoude@126.com (J. Shi), blci@163.com (L. Bai).
[1] These authors contributed equally to this work.

https://doi.org/10.1016/j.cclet.2022.05.089
1001-8417/

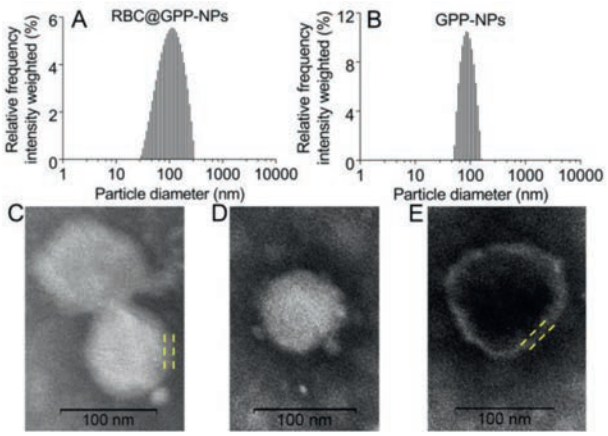


**Fig. 1.** Characterization of nanoparticles. (A) Size distribution of RBC@GPP-NPs. (B) Size distribution of GPP-NPs. (C) TEM image of RBC@GPP-NPs. (D) TEM image of GPP-NPs. (E) TEM image of erythrocyte membrane vesicles. The yellow dashed lines show the thickness of RBCM. The scale bars = 100 nm.

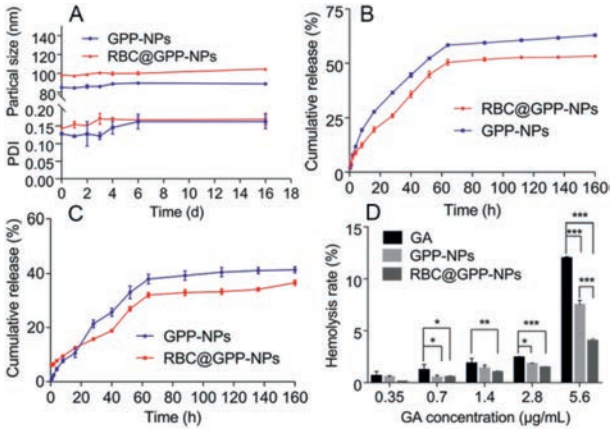


**Fig. 2.** (A) Stability of GPP-NPs and RBC@GPP-NPs. Drug release of GPP-NPs and RBC@GPP-NPs at pH 5.5 (B) and pH 7.4 (C). (D) Hemolysis assay of GPP-NPs and RBC@GPP-NPs. Data were presented as the mean ± SD ($n = 3$). $^{*}P < 0.05$; $^{**}P < 0.01$; $^{***}P < 0.001$.

gambogic acid) [26,27] or synthetic compounds (sorafenib) [28]. And the cell membrane nanotechnology has achieved breakthrough development in the past five years, which organically combines bionic technology and nanotechnology to improve therapeutic effect of drugs. Moreover, the RBCM can be further modified to favor its targeting functions since its surface contains diversified functional groups [29].

Herein, we built a biomimetic nanocarrier based on the RBCM, specifically by wrapping GA in the polymer mPEG-PLA to form nanoparticles (GPP-NPs) and mimicking it with RBCM to obtain RBC@GPP-NPs to overcome these shortcomings of GA and improve its antitumor activity. After that, we performed a series of characterization experiments to identify the physicochemical properties of GPP-NPs and RBC@GPP-NPs. The results obtained through membrane dialysis methods (DLS) showed that RBC@GPP-NPs and GPP-NPs were narrow and monodisperse and owned the averages of particle size were about 102.3 ± 3.1 nm (Fig. 1A) and 89.55 ± 0.92 nm (Fig. 1B), respectively. Noticeably, the increment in diameter is approximately equals to the thickness of RBCM, which is about 12 nm [30]. And the average particle size of GPP-NPs was within the range of what the membrane cloaking approach could be applied to [31]. The transmission electron microscopy (TEM) results showed that RBC@GPP-NPs (Fig. 1C) and GPP-NPs (Fig. 1D) were all uniformly distributed spherical NPs. Besides, RBC@GPP-NPs had an outer membrane with the same thickness as the RBCM (Fig. 1E). The encapsulation efficiency (EE) of RBC@GPP-NPs and GPP-NPs were (79.11 ± 1.42)% and (86.37 ± 0.84)%, respectively, indicating that RBCM-coated NPs could efficiently load GA.

Next, to test the stability of RBC@GPP-NPs, we recorded their changes of size and PDI in PBS within 17 days at 4 °C. As shown in Fig. 2A, at day 6, the particle size of RBC@GPP-NPs increased from an average diameter of 98.35 nm to 100.06 nm with an increment of 1.71 nm, and the size of GPP-NPs increased from 85.01 nm to 89.7 nm, the increment was 4.69 nm. This led to the fact that both two NPs were stability with 6 days, but RBC@GPP-NPs performed better. After 16 days their increments were both less than 7 nm, yet the increment of membrane-free NPs was lower than RBC@GPP-NPs. Additionally, the PDI values of both groups converged to 0.15 after day 6, which indicated that they both had good dispersion. To predict the release behavior of nanoparticles *in vivo*, we investigated their drug release characteristics of at pH 7.4 and pH 5.5. In neutral medium (pH 7.4), the maximum cumulative GA release rate of RBC@GPP-NPs was about 36.62%, which was lower than that of GPP-NPs (41.44%). While in acidic medium (pH 5.5), the maximum GA cumulative release rate of RBC@GPP-NPs increased to 53.25%, which was still lower than the drug release rate of GPP-NPs (62.96%). And the results of Figs. 2B and C showed that the drug release of RBC@GPP-NPs and GPP-NPs both had higher release in acidic environment than neutral environment; RBC@GPP-NPs could delay the release of GA, and its continuous and stable slow-release behavior would increase the accumulation of drug in the tumor environment while reducing the side effects [32,33]. These results expressed that RBCM coated NPs have the potential to maintain effective drug concentrations *in vivo* where the RBCM acts as a physical barrier to NPs [34].

To investigate the blood biocompatibility of RBC@GPP-NPs, we moved on to carry out the hemolysis assay experiments. Fig. 2D shows that the hemolysis ratio (HR) of GPP-NPs was slightly hemolyzed at a maximum drug concentration of 5.6 g/mL, whereas the HR of free GA was nearly 12%. The hemolytic results of RBC@GPP-NPs, on the other hand, were much lower and negligible (<5%), indicating that RBC@GPP-NPs were safe for blood system.

To evaluate the whether the RBC@GPP-NPs could reserve the anti-tumor activity of GA against HepG2, we used 3-(4,5-dimethylthiazol-2-y1)-2,5-diphenyl-2*H*-tetrazolium bromide (MTT) assay to check cell viability. Normal cell line (L02 cells) was used to appraise the safety of nanoparticles. All pharmaceutical agents were detected to have both a dose- and time-dependent cytotoxicity to HepG2 cells after 24 and 48 h of incubation. The results after 24 h demonstrated no distinction between the three groups on HepG2 cells (Fig. 3A). However, a notable phenomenon was that the cell viability of RBC@GPP-NPs rapidly decreased from 90% to 30% at GA concentrations of 0.35–1.4 μg/mL (Fig. 3B), which was twice as much as the other two groups. This was probably in response to the improved controlled drug release effect of RBC@GPP-NPs.

Apart from that, we examined the cytotoxicity of GA loaded nanoparticles on normal cells by MTT method. The results confirmed that RBC@GPP-NPs and GPP-NPs can both decrease the cytotoxicity of L02 cells when compared to free GA. And the erythrocyte membrane-encapsulated bionic nanoparticles have the highest safety profile. After 24 h, the cell survival rate of L02 cells was almost 100% at low drug concentrations (0.35–2.8 μg/mL) of RBC@GPP-NPs, and the GPP-NPs group was the second highest (Fig. 3C); after 48 h, the cell survival rate of RBC@GPP-NPs was significantly higher than that of GPP-NPs and free GA group (Fig. 3D), indicating that RBCM could enhance the biocompatibility of RBC@GPP-NPs. These were consistent with the results of previous studies [35].

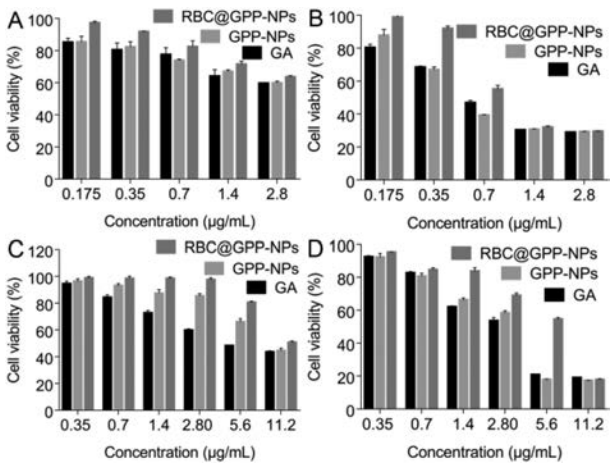


**Fig. 3.** *In vitro* evaluation of anticancer activity of nanoparticles. HepG2 cell survival ratio after treatment with different types of GA at various concentrations for 24 h (A) and 48 h (B). Cell survival ratio of L02 cells after treated with different types of GA for 24 h (C) and 48 h (D).

After verifying the potential antitumor activity of RBC@GPP-NPs *in vitro*, we proceeded to discuss their antitumor efficacy in tumor-bearing mice. The protocols for animal assays were approved by Institutional Animal Care and Ethics Committee of Sichuan Provincial People's Hospital (No. 2017050009). The main experimental flow was given in Fig. 4A, and all mice were dissected under ether anesthesia (Fig. 4B). As shown in Fig. 4C, the RBC@GPP-NPs group showed the slowest increase in tumor volume with a mean volume of 715 $mm^3$. After the last treatment with saline, GA and GPP-NPs, the tumor volume of mice increased to approximately 1138 $mm^3$, 920 $mm^3$ and 922 $mm^3$, respectively after 16 days from the first injection, indicating that the dose of 2 mg/kg did not achieve the effective concentration of tumor growth inhibition. Photographs of tumor tissue in different groups were shown in Fig. S1 (Supporting information). The enhanced anti-tumor function may be due to the remarkable increase of GA circulation time in mice by the bionic nanoparticles [36]. Besides, the H&E results supported the above results that RBC@GPP-NPs exhibited the strongest tumor growth inhibition as they resulted in more extensive apoptosis in tumor tissues compared to the GPP-NPs group and free GA group (Fig. 4D). Together, these results validated that RBC@GPP-NPs could promote anti-tumor activity of GA for sustained treatment of HCC.

In addition to favorable antitumor efficacy, RBC@GPP-NPs also provided a high *in vivo* safety profile. As shown in Fig. S2A (Supporting information), the body weight of mice in the RBC@GPP-NPs, GPP-NPs, free GA and saline groups had no significant differences. The major organ coefficients were normal in all groups with no significant differences (Fig. S2B in Supporting information). In top of that, there were no abnormal expression in ALT (alanine aminotransferase), AST (aspartate aminotransferase), CREA (creatinine), and UA (uric acid) levels between whatever medication administration group or control group, indicating that liver and kidney functions were not impaired in all groups (Fig. S2C in Supporting information). Meanwhile, H&E-stained images of major organs in each group suggested non-obvious organ damage in all groups (Fig. S2D in Supporting information), suggesting a good biocompatibility of RBC@GPP-NPs. Taken together, the results suggested that RBC@GPP-NPs displayed enhanced anti-tumor activity, good biocompatibility and safety, high stability, and increased water solubility, therefore were promising for future clinical applications.

In conclusion, we have successfully constructed novel erythrocyte membrane-based mimetic gambogic acid-loaded nanoparti-

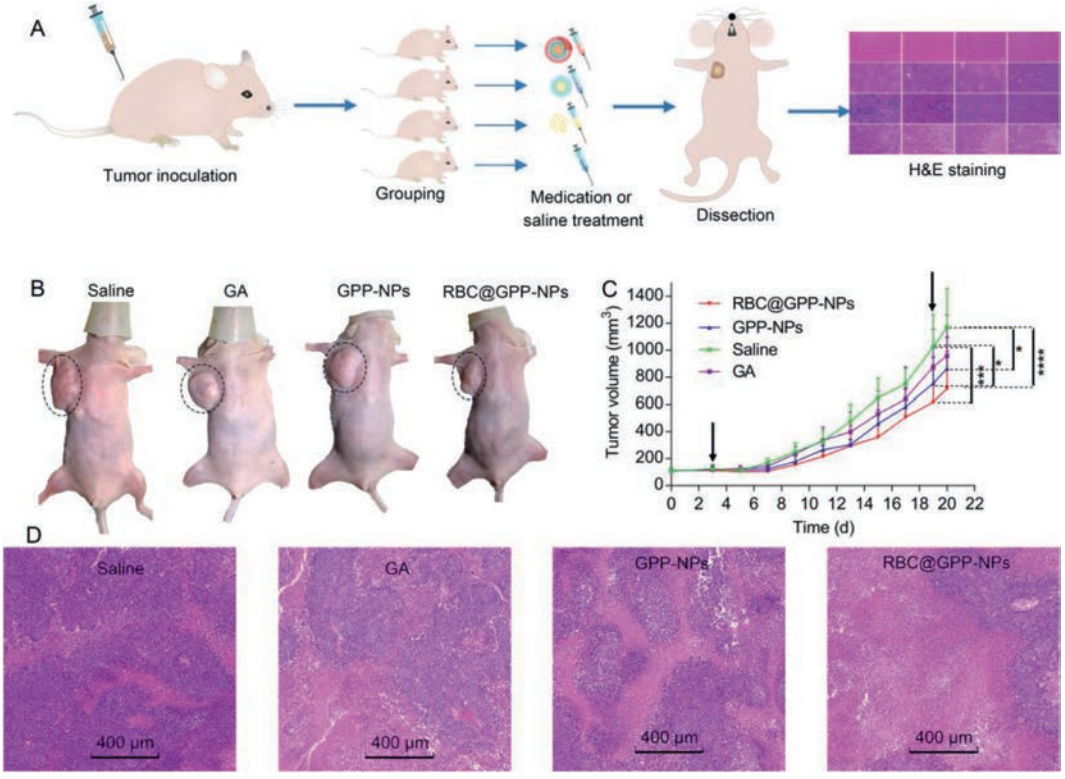


**Fig. 4.** *In vivo* antitumor efficacy of RBC@GPP-NPs. (A) Animal experiments procedure. The groups and therapeutic agents from top to bottom are RBC@GPP-NPs, GPP-NPs, free GA and saline ($n = 6$). The blue arrows indicate the direction of experimental progress. (B) Nude mice were dissected under ether anesthesia; tumors on the right axilla of nude mice were exhibited with a black oval dotted line for the four groups. (C) Changes in tumor volume growth of each group, the black arrow on the left represents the first dose and the right represents the last dose. (D) Histological analyses of tumor sections after various treatments by H&E staining, scale bars indicate 400 μm. $^{*}P < 0.05$; $^{**}P < 0.01$; $^{***}P < 0.001$, $^{****}P < 0.0001$.

cles (RBC@GPP-NPs), which exhibited good stability, long *in vitro* release time and good biosafety, and demonstrated effective HepG2 inhibitory activity *in vitro* and the most potent antitumor activity *in vivo*. We created a new type of membrane-encapsulated nanoparticles (RBC@GPP-NPs) with a core-shell structure by co-extruding the RBCM shell and the GA-loaded polymeric NPs core. Our studies revealed that RBCM not only enhanced the biocompatibility of RBC@GPP-NPs compared with single GPP-NPs, but also produced stronger antitumor activity *in vivo* while ensuring the safety of systemic administration. Therefore, this study is instructive for any further research of GA's nano-formulations.

## Declaration of competing interest

No potential conflict of interest was reported by the authors.

## Acknowledgments

This work was supported by the National Natural Science Foundation of China (No. 81900339), Key Research and Development Program of Science and Technology Department of Sichuan Province (No. 2019YFS0514) and Health Commission of Sichuan Province (No. 20PJ095).

## Supplementary materials

Supplementary material associated with this article can be found, in the online version, at doi:10.1016/j.cclet.2022.05.089.

## References

[1] A. Hefnawy, I.H. Khalil, K. Arafa, M. Emara, I.M. El-Sherbiny, Int. J. Nanomed. 15 (2020) 821–837.
[2] H. Sung, J. Ferlay, R.L. Siegel, et al., CA: Cancer J. Clin. 71 (2021) 209–249.
[3] J. Ferlay, M. Colombet, I. Soerjomataram, et al., Int. J. Cancer 149 (2021) 778–789.
[4] T. Sun, Y.S. Zhang, B. Pang, et al., Angew. Chem. Int. Ed. 53 (2014) 12320–12364.
[5] D.A. Dias, S. Urban, U. Roessner, Metabolites 2 (2012) 303–336.
[6] P.N.H. Lee, W.S. Ho, Oncol. Rep. 29 (2013) 1744–1750.
[7] M.S. Park, N.H. Kim, C.W. Kang, C.W. Oh, G.D. Kim, Drug. Dev. Res. 76 (2015) 132–142.
[8] Z. Ke, L. Yang, H. Wu, et al., Int. J. Pharm. 545 (2018) 306–317.
[9] E. Hatami, M. Jaggi, S.C. Chauhan, M.M. Yallapu, Biochim. Biophys. Acta Rev. Cancer 1874 (2020) 188381.
[10] Y. Wang, X. Wang, J. Zhang, et al., Chin. Chem. Lett. 30 (2019) 885–888.
[11] L. Wu, H. Guo, H. Sun, et al., Anti-Cancer Drugs 27 (2016) 988–1000.
[12] K. Hao, X.Q. Liu, G.J. Wang, X.P. Zhao, Eur. J. Drug Metab. Pharmacokinet. 32 (2007) 63–68.
[13] L. He, Y. Ling, L. Fu, et al., Bioorg. Med. Chem. Lett. 22 (2012) 289–292.
[14] E. Blanco, T. Sangai, A. Hsiao, et al., Cancer. Lett. 334 (2013) 245–252.
[15] L. Cai, N. Qiu, M. Xiang, et al., Int. J. Nanomed. 9 (2014) 243–255.
[16] S. Adepu, H. Luo, S. Ramakrishna, Int. J. Mol. Sci. 22 (2021) 5433.
[17] S. Acharya, S.K. Sahoo, Adv. Drug Delivery Rev. 63 (2011) 170–183.
[18] P.A. Gunatillake, R. Adhikari, Eur. Cells Mater. 5 (2003) 1–16.
[19] W. Pei, B. Huang, S. Chen, et al., Int. J. Nanomed. 15 (2020) 10151–10167.
[20] Y. Wang, K. Zhang, T. Li, et al., Theranostics 11 (2021) 164–180.
[21] Q. Zhao, X. Sun, B. Wu, et al., J. Nanobiotechnol. 19 (2021) 8.
[22] E.T. Dams, P. Laverman, W.J. Oyen, et al., J. Pharmacol. Exp. Ther. 292 (2000) 1071–1079.
[23] D. Dehaini, X. Wei, R.H. Fang, et al., Adv. Mater. 29 (2017) 1606209.
[24] M. Bhateria, R. Rachumallu, R. Singh, R.S. Bhatta, Expert. Opin. Drug. Deliv. 11 (2014) 1219–1236.
[25] Y. Mao, C. Zou, Y. Jiang, D. Fu, Chin. Chem. Lett. 32 (2021) 990–998.
[26] Z. Zhang, H. Qian, M. Yang, et al., Int. J. Nanomed. 12 (2017) 1593–1605.
[27] C. Guo, X. Hou, Y. Liu, et al., Phytomedicine 80 (2021) 153356.
[28] Z. Li, G. Yang, L. Han, et al., J. Nanobiotechnol. 19 (2021) 360.
[29] L.M. Bush, C.P. Healy, S.B. Javdan, J.C. Emmons, T.L. Deans, Trends. Pharmacol. Sci. 42 (2021) 106–118.
[30] Z. Zhang, H. Qian, J. Huang, et al., Int. J. Nanomed. 13 (2018) 4961–4975.
[31] B.T. Luk, C.M.J. Hu, R.H. Fang, et al., Nanoscale 6 (2014) 2730–2737.
[32] K. Ou, X. Xu, S. Guan, et al., Adv. Funct. Mater. 30 (2020) 1907857.
[33] X. You, L. Wang, L. Wang, J. Wu, Adv. Funct. Mater. 31 (2021) 2100805.
[34] C. Jiménez-Jiménez, M. Manzano, M. Vallet-Regí, Biology (Basel) 9 (2020) 406.
[35] L. He, T. Nie, X. Xia, et al., Adv. Funct. Mater. 29 (2019) 1901240.
[36] X. Liu, X. Zhong, C. Li, Chin. Chem. Lett. 32 (2021) 2347–2358.